OPEN ACCESS Freely available online

Journal of Physical Chemistry & Biophysics

Research Article

Photocatalytic Degradation Studies of Indigo Carmine Dye by Green-Synthesized Silver Nanoparticles from *Theobroma cacao* Extracts

Oyewole TS[1], Olowu RA[1*], Osundiya MO[1], Tovide OO[1], Akanbi PJ[1], Abosede SO[1], Ejire AA[2]

[1]*Department of Chemistry, Lagos State University, LASU Ojo, Nigeria;* [2]*Department of Chemistry, Lagos State University of Science and Technology, Ikorodu, Nigeria*

ABSTRACT

The breakdown of dyes poses a considerable problem due to their enduring and resilient characteristics; as a result, creating materials with suitable properties for dye decomposition is a crucial research focus. This study focused on creating Silver Nanoparticles (Ag NPs) utilizing environmentally friendly synthesis techniques and non-toxic *Theobroma cacao* extract. Various analytical methods, including UV-visible spectroscopy, XRD, FTIR, TEM, BET, and SEM/EDX, were employed to verify the formation of Ag NPs. The produced Ag NPs exhibited a characteristic peak at 420 nm in the UV-visible spectrum. XRD analysis confirmed the crystalline structure of the nanoparticles, which had an average size of 12.78 nm. The XRD pattern showed peaks at 34.2, 37.9, 44.2, and 64.6°, corresponding to the (100), (111), (200), and (220) planes of the Face-Centered Cubic (FCC) silver crystal structure. FTIR results indicated that the extracts containing O-H functional groups played a role in capping the nanoparticle synthesis. TEM analysis revealed that the nanoparticles had a size distribution ranging from 9.22 nm to 52.60 nm in diameter. The BET method determined that the synthesized nanoparticles possessed a surface area of 15.52 m^2/g and a pore diameter of 2.105 nm. SEM examination at various magnifications showed that the nanoparticles had a rough surface texture with imperfections such as cracks or voids. EDX analysis demonstrated that silver was the primary element in the nanoparticles, comprising 79.93% of their composition. The study also explored the photocatalytic performance of the Ag nanoparticles in degrading indigo carmine dye under UV light exposure. According to the results, Ag NPs exhibited a maximum removal efficiency of 80.2% in 75 min. This demonstrated that the synthesized Ag nanoparticles possess strong potential for application as photocatalysts to rapidly degrade industrial dyes in water treatment.

Keywords: Green synthesis; Indigo carmine dye; Photodegradation; *Theobroma cacao*; Water remediation

INTRODUCTION

Acid Blue 74, also known as indigo carmine, is a synthetic colorant widely employed in diverse industries, including textiles, food, and pharmaceuticals [1]. The global issue of water contamination by indigo carmine is of significant concern due to its detrimental effects on human health and aquatic life [2]. indigo carmine dye is commonly used in many fields such as the textile, food, pharmaceutical, printing, and leather industries. Water contamination by indigo carmine is a global problem due to its negative effects on human health and the aquatic environment. For example, the presence of indigo carmine in the aquatic environment reduces light penetration, which negatively affects photosynthesis. Indigo carmine ingestion by Humans causes skin and eye irritations, difficulty breathing, and can damage the neurological system. However, indigo carmine removal from wastewater is important. Thus, several methods such as filtration, electrocoagulation processes, oxidation, and adsorption have been developed to treat dyestuffs wastewater This dye's presence in water bodies reduces light penetration, thereby impeding photosynthesis. Human contact with indigo carmine may lead to skin and eye irritation, breathing difficulties

Correspondence to: Olowu RA, Department of Chemistry, Lagos State University, LASU Ojo, Nigeria; E-mail: toyib.oyewole@lasu.edu.ng

Received: 11-Apr-2025, Manuscript No. JPCB-25-37256; **Editor assigned:** 15-Apr-2025, PreQC No. JPCB-25-37256 (PQ); **Reviewed:** 29-Apr-2025, QC No JPCB-25-37256; **Revised:** 11-Jun-2025, Manuscript No. JPCB-25-37256 (R); **Published:** 18-Jun-2025, DOI: 10.35841/2161-0398.25.15.422

Citation: Oyewole TS, Olowu RA, Osundiya MO, Tovide OO, Akanbi PJ, Abosede SO, et al. (2025) Photocatalytic Degradation Studies of Indigo Carmine Dye by Green-Synthesized Silver Nanoparticles from *Theobroma cacao* Extracts. J Phys Chem Biophys. 15:422.

[2], and possible neurological damage [3]. The introduction of indigo carmine into aquatic environments can result in substantial color pollution, obstructing light penetration and disrupting aquatic ecosystems [4]. This dye has the potential to harm aquatic organisms, possibly causing disturbances in the food chain and diminishing biodiversity [5]. Insufficiently treated effluents from dye industries can create an imbalance in ecosystem oxygen levels by reducing dissolved oxygen. Moreover, these effluents hinder sunlight penetration, altering the environment's photosynthetic activity. This leads to a deterioration in water quality and subsequent harmful effects on local plant and animal life [6]. Considering the negative impacts of artificial dyes on ecosystems and human well-being, the elimination of these substances from industrial wastewater and polluted water sources has become increasingly vital [7]. Although indigo carmine serves important functions in its intended applications, its release into the environment raises serious concerns due to its persistence and potential to harm aquatic communities and human health [8].

Silver (Ag) stands out amongst the metal oxides and metal Nanoparticles (NPs) currently under scientific investigation. Ag NPs exhibit distinctive properties, including catalytic capabilities, photochemical characteristics, therapeutic effects, fungicidal and antimicrobial activities, and UV filtration abilities. These features render them versatile and particularly apt for wastewater treatment [9]. While various techniques exist for Ag NP production, such as substance, snowfall, hydrothermal, microwave, solvothermal, and vibration methods, biosynthetic approaches are gaining traction due to their advantages over traditional techniques [10,11]. Utilizing plant materials in biosynthesis is especially advantageous, as it eliminates the need for complex cell culture maintenance and markedly reduces reaction time from days to hours [12]. Moreover, the integration of plant material components with nanoparticles not only stabilizes the system but also introduces biocompatible functionalities, enhancing biological interactions. Green-synthesized Ag NPs have wide-ranging applications, serving as optical receptors for solar energy absorption, catalysts in chemical reactions, bio-labelling agents, and antimicrobial substances [13]. Prior research has demonstrated that Ag NPs produced using plant-based extracts have potential medical applications. Recently, the bio-components of various plant extracts have been identified as effective agents for synthesizing metal nanoparticles. As a result, researchers globally are exploring plant extract biomolecules to control nanoparticle size, shape, and stability. The biosynthesis of Ag NPs has been investigated using several plants, including *Malva parviflora* [14], *Aggregatimonas sanguine* [15], and *Lantana camara* [16]. Antioxidant-containing extracts from different plant parts, such as leaves, roots, seeds, stems, and fruits, have been examined for Ag NP biosynthesis. The biologically inspired green synthesis of Ag NPs is evolving into a distinct and significant branch of nanotechnology [17]. In comparison to conventional physical and chemical methods, green synthesis of nanoparticles using microorganisms, enzymes [18], and plant extracts [19] offers numerous benefits [19]. Biological synthesis routes are cost-effective, environmentally friendly, easily scalable for large-scale production, and do not require toxic chemicals, high pressure, temperature, or energy, thus enhancing their medical applicability [20,21]. The use of plant materials offers greater advantages compared to other biological methods, as it eliminates the requirement for cell culture maintenance and shortens reaction times from days to mere hours. Integrating plant-derived elements with nanoparticles not only imparts stability to the system but also introduces biocompatible characteristics to these NPs, improving their biological interactions. Significant research has been devoted to the application of plant extracts in producing noble metal nanoparticles, with a particular emphasis on Silver Nanoparticles (AgNPs). The attractiveness of plant extract techniques stems from their straightforward nature, cost-efficiency, and environmental friendliness, yielding nanoparticles with unique properties applicable across various sectors including biomedicine, fiber technology, electronics, food preservation, cosmetics, and others [22].

Theobroma cacao L. (*T. cacao*), a perennial tree crop widely grown in West Africa and South America, boasts numerous industrial uses and is recognized for its polyphenols, which possess strong antioxidant and antimicrobial properties. Preliminary phytochemical analyses have revealed the existence of various compounds, including saponins, tannins, glycosides, triterpenoids, sterols, coumarins, flavonoids, and alkaloids. Processed cocoa leaf extracts are abundant in antioxidants, which can serve as natural antimicrobials and antioxidants [21]. The biochemical composition of *T. cacao* L. is multifaceted, encompassing alkaloids (theobromine and caffeine), polyphenols (flavonoids and anthocyanins), tannins, amino acids, vitamins (C and E), minerals (magnesium, potassium, calcium), terpenoids, carbohydrates, lipids, proteins, and organic acids. These constituents synergistically deliver health benefits, such as antioxidant, anti-inflammatory, cardiovascular, and neuroprotective effects. Owing to their bioactive characteristics, cocoa leaves are highly valued in the pharmaceutical, nutraceutical, and cosmetic sectors, offering remedies for cardiovascular diseases, neurodegenerative disorders, and metabolic syndromes, as well as functioning as dietary supplements and skincare products. The complex chemical profile of cocoa leaves highlights their potential applications across various industries [23].

Silver Nanoparticles (AgNps) stand out among metallic nanoparticles for their diverse applications in biological and environmental fields. These nanoparticles excel at breaking down various dyes. While Ag Nps can be manufactured through physical and chemical processes, these methods are often costly or involve harmful chemicals. Consequently, there is a demand for eco-friendly production techniques that avoid hazardous substances. Green synthesis of AgNps represents a rapidly growing and cost-effective approach in nanoparticle production. Numerous plant extracts serve as both capping and reducing agents in nanoparticle synthesis, eliminating the need for dangerous chemical agents and complex purification methods. Examples of plants used in this process include *Azadirachta indica*, *Catharanthus roseus*, *Phoma glomerata*, *Cissus quadrangularis*, *Elettaria cardamom*, *Lantana camara* flower, *Andean blackberry* leaf, *Nephelium lappaceum* peel, and clove extract.

To the best of the researcher's knowledge, there have been no reported attempts to make use of the considerable amount of discarded *Theobroma cacao* leaves. This research aims to investigate the photocatalytic degradation of indigo carmine dye using green-synthesized silver nanoparticles from *Theobroma cacao* extracts. The synthesized Ag NPs are extensively characterized using various analytical methods. This paper presents a straightforward, scalable, and efficient approach for producing Ag nanoparticles from waste *Theobroma cacao* leaves. Furthermore, it examines the potential uses of these Ag NPs by evaluating their effectiveness in breaking down indigo carmine dye in artificial wastewater through photodegradation.

MATERIALS AND METHODS

Chemicals and plant material collection

Theobroma cacao leaves are harvested from farmland in the Igando-Egan area of Alimosho, Lagos State, Nigeria, for various purposes. The harvesting process adheres to stringent quality standards. A botanist from an Agricultural University authenticated and confirmed the leaves' identity. Reagents of analytical grade were obtained and used without further refinement. Silver Nitrate ($AgNO_3$), with a purity of ≥ 99.5%, was sourced from Sigma-Aldrich in India. All solutions were formulated, diluted, and rinsed using double-distilled water.

Biosynthesis of Ag NPs

The harvested *Theobroma cacao* leaves were thoroughly cleaned with distilled water and air-dried at ambient temperature for 10 days to remove any remaining moisture. Subsequently, the dried leaves were ground into a fine powder using a sterile electric blender and stored in an airtight container away from sunlight for later use. In a 1000 ml Erlenmeyer flask, 20 g of the leaf powder was mixed thoroughly with 400 ml of distilled water. This mixture was then heated on a magnetic stirrer at 60°C for 2 hours with constant agitation, resulting in a light yellow liquid at ambient temperature during the boiling process. The yellow extract was further refined using Whatman No. 1 filter paper and stored in a freezer.

A 0.01 M Silver Nitrate ($AgNO_3$) solution was prepared and heated to 60°C under stirring conditions on a magnetic stirrer to synthesize silver nanoparticles. Then, 20 mL of the *T. cacao* extract was introduced to the mixture. After 5 minutes, 1 M of NaOH aqueous solution was added dropwise to adjust the pH to alkaline. The reduction of silver ions occurred quickly, as indicated by the solution turning dark brown within 10 minutes, confirming the formation of Ag NPs. No further color changes were observed [24]. The resulting Ag NPs were purified through multiple rounds of centrifugation at 20,000 rpm for 20 minutes, followed by re-suspension of the pellet in distilled water to remove water-soluble biomolecules such as proteins and secondary metabolites. Finally, the Ag NPs were collected and transferred to a clean bottle for further analysis. Figure 1 shows the graphical representations of the biosynthesis of Ag NPs.

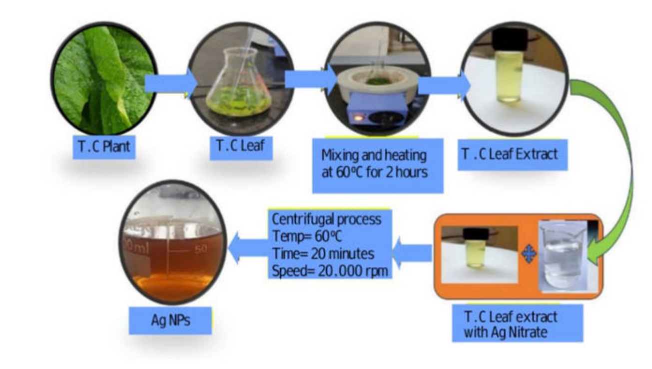

Figure 1: Biosynthesis process of Ag NPs from T.C leaf.

Photocatalytic experiments

The degradation of Indigo Carmine Dye (ICD) was evaluated using photocatalytic Ag NPs, with a UV-visible light source (average solar flux of 500 km $h^{-1}m^{-2}$) and a distance of 21 cm between the light source and the pollutant solution. The reaction was initiated by adding 10 mg of Ag NPs to a 10 ppm solution (10 mg L^{-1}) of the dye and stirring the mixture for 75 minutes in the dark to establish an adsorption-desorption equilibrium. Afterward, the mixture was stirred under UV irradiation, and 2 mL of the suspension was withdrawn every 15 minutes for up to 75 minutes to measure the absorption peak. The absorbance was measured at the maximum absorbance wavelength of the dye, typically at 610 nm which was considered the absorption of the dye at a given time (t) and analyzed using UV-Vis spectroscopy. The following equation was used to determine the dye degradation [25].

$$\textbf{Degradation (\%)} = \frac{(C0-Ct)}{C0} \times 100 \qquad (1)$$

Where C_0 is the Concentration at time=0 and C_t is the concentration at time=t.

Kinetic analysis: A plot of the natural logarithm of the concentration ratio of (In Co/Ct) versus time to determine the reaction kinetics, often fitting to a first-order kinetic model.

$$In\frac{Co}{Ct} = kt \qquad (2)$$

Where k is the rate constant.

Characterization of the synthesized AgNPs

The synthesized AgNPs were characterized by various instrumental analyses. XRD (X-Ray Diffraction) images were captured using Cu K (k=0.152) illumination and a Siemens D5005 diffractometer. Maximal peak locations were contrasted using standard information to determine the crystallographic stage. Fourier Transform Infrared spectroscopy (FT-IR) of the freeze-dried samples was recorded with ATR-FTIR using (Bruker Vertex-80 spectrometer) was employed to identify the chemical molecules that coated the Ag NPs. The average particle size was obtained from TEM analysis using FE-TEM with Tecnai TF30 ST at an accelerating voltage of 300 kV. UV–vis spectroscopy measurements were recorded on a Perkin Elmer Lambda 950 UV–vis-NIR spectrophotometer with a wavelength resolution better than ± 0.2 nm. Brunauer-Emmett-Teller (BET) was employed to measure the surface area, pore size, and pore diameter of the synthesized Ag NPs. Employing the field emission Scanning Electron Microscope (SEM), (FEG-SEM; JEOL/JEM-1230) the specimen's structure, geography, and dimension were determined.

RESULTS AND DISCUSSION

UV-vis absorption spectroscopy analysis

The absorption spectra of green synthetic Ag NPs, as illustrated in Figure 2, exhibit a peak at approximately 420 nm. This observation suggests that the elevated excitation bonding energy of Ag NPs at ambient temperature results in their excitation absorption at this wavelength. Additional evidence indicates a slight blue shift in the Ag NPs' absorption spectrum between 400 and 440 nm. UV-vis spectral analysis confirmed an inverse correlation between extracted quantity and particle size. These findings are consistent with previous research on nanoparticle size variations [26]. The blue shift in the absorption edge is attributed to the quantum confinement effect among individual particle sizes [27]. The calculated band gap for Ag NPs synthesized using *T. cacao* leaf extract indicates semiconductor-like properties. This band gap value enables the Ag NPs to absorb visible light, which is essential for various applications such as photocatalysis, sensors, and optoelectronic devices. The phytochemicals present in *T. cacao* leaf extract, including flavonoids and phenolic compounds, are hypothesized to play a role in reducing and stabilizing silver ions during synthesis, thereby influencing the electronic properties of the resulting nanoparticles [28].

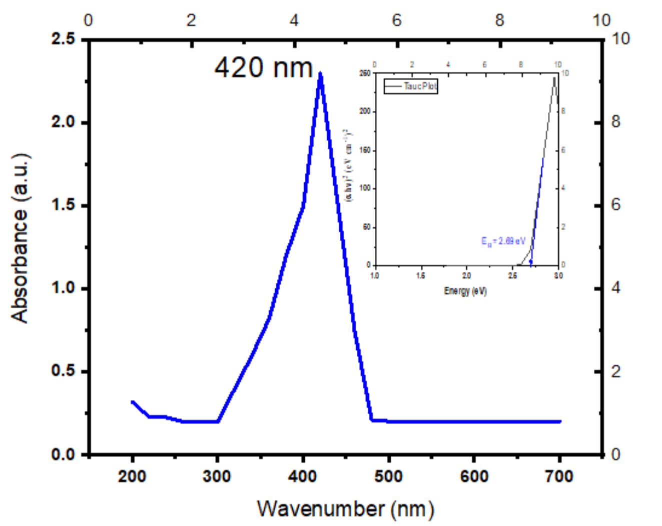

Figure 2: UV-spectra analysis of biosynthesized Ag NPs and Tauc plot.

X-ray diffraction (XRD) analysis

The XRD analysis reveals prominent Ag NPs peaks at 34.2, 37.9, 44.2, and 64.6°, corresponding to the (100), (111), (200), and (220) planes of the Face-Centered Cubic (FCC) silver crystal structure, as shown in Figure 3. The four planes align perfectly with JCPDS card 04-0783 parameters. These observations confirmed that Ag NPs exhibited a face-centered cubic structure. The (111) orientation exhibits the highest intensity, indicating its predominance. The Ag NP crystallite size is determined using Debye-Scherrer's formula [29].

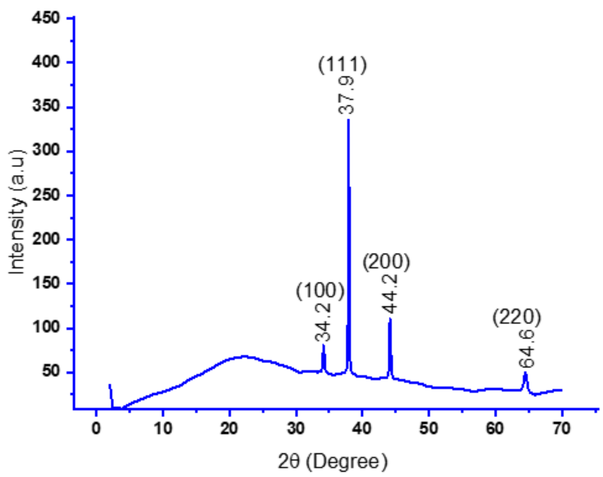

Figure 3: X-ray diffraction pattern of the biosynthesized silver nanoparticles.

$$D = \frac{K\lambda}{\beta \cos\theta} \quad (3)$$

Where D denotes the average crystallite size, K Scherer's constant (K=0.94), λ X-ray wavelength (0.1546 nm), β full-width at half-maximum of diffraction line in radians, and θ half diffraction angle. Applying this formula, the crystallite's size is 12.78 nm.

Fourier Transform Infrared Spectroscopy (FT-IR) analysis

FTIR spectroscopy serves as a valuable analytical tool for examining potential interactions between Ag NPs and various functional groups present in the plant extract of *Theobroma cacao*. The FTIR spectrum reveals the presence of different functional groups at distinct positions (Figure 4). The peak at 3608.5 cm^{-1} observed in the plant extract of sample is attributed to the O-H stretching vibration of phenolic groups. An increase in the peak intensity is observed due to the coordination of Ag^+ (3619.7 cm^{-1}) and surface interaction with the hydroxyl group, which can enhance the availability for other reactions. The bands appearing at 3336.7, 3332.9, 3042.6, and 3038.8 cm^{-1} can be attributed to N–H stretching in primary aromatic amines bonds of aromatic in flavonoid molecules in the plant extract of *Theobroma cacao*. A strong band at 1728.3 cm^{-1} is attributed to carbonyl groups involved in nanoparticle formation [30,31].

less intense band at 3332 cm^{-1} is assigned to N–H stretching in primary aromatic amines [32]. The sharp peak at 3031 cm^{-1} indicates C-H stretching of alkene, while a weak peak at 2554.8 cm-1 is associated with S-H stretching of thiol. The broad peak at 1359.7 cm-1 can be linked to the O-H bending of alcohol. These peaks suggest that phenolic compounds and other phytochemicals in *T. cacao* contribute to the reduction and stabilization of Ag NPs. The FTIR analysis indicates that hydroxyl and carbonyl groups in carbohydrates, flavonoids, terpenoids, and phenolic compounds function as potent reducing agents, potentially facilitating the bioreduction of Ag^+ ions to Ag^0 nanoparticles. Furthermore, the analysis confirms that carbonyl groups of amino acid residues and peptides in proteins exhibit a strong affinity for metal ions, possibly encapsulating the nanoparticles and forming a protective membrane to prevent agglomeration, thus stabilizing the nanoparticles in the medium. Notably, the leaf extracts specifically influenced the nanoparticle size, inhibiting oxidation of the Ag NPs. In this process, proteins and secondary metabolites from the extract play a crucial role in nanoparticle formation's reducing and capping mechanisms.

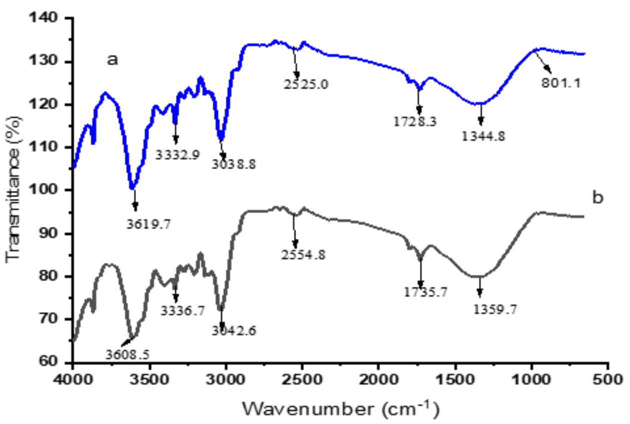

Figure 4: FT-IR analysis of (a) biosynthesized Ag NPs (b) plant extract of *Theobroma cacao*.

Brunauer-Emmett-Teller (BET) analysis

BET revealed that synthesized nanoparticles' surface area, pore volume, and pore diameter were 15.52 m^2/g, 0.272 cm^3/g, and 2.105 nm respectively. Using the Brunauer-Emmett-Teller (BJH) method, according to the IUPAC porosity classification, the synthesized Ag NPs are mesoporous. Mesophorus particles are particles ranging from 2 to 50 nm in size. Since the synthesized AgNPs have a pore diameter of 2.105 nm, it is therefore classified as a mesoporous particle (Figure 5).

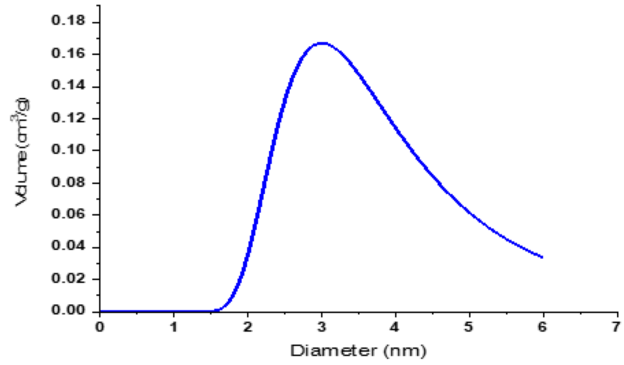

Figure 5: The pore size distribution of synthesized Ag NPs.

Scanning Electron Microscope (SEM) analysis

The Scanning Electron Microscopy (SEM) images (Figures 6a and b) display the structure of Ag NPs at various magnifications, showing an uneven surface texture with imperfections like fissures or cavities. The consistent shape observed in both images indicates a uniform distribution of particle size, which is attributed to the magnetic interactions between individual silver nanoparticles [33]. The EDX analysis of the biosynthesized silver nanoparticles was conducted to evaluate the composition of the active components present in the sample. The EDX images are presented in Figure 7. The results shown in Figure 7 and Table 1 indicate that the biosynthesized particles comprised silver as the major element (79.93%) The uniform dispersion formation can also be explained by the presence of biological compounds from theobroma cacao on the nanoparticle surfaces. Additionally, the theobroma cacao biomolecules may contribute to the increased stability of Ag NPs [29].

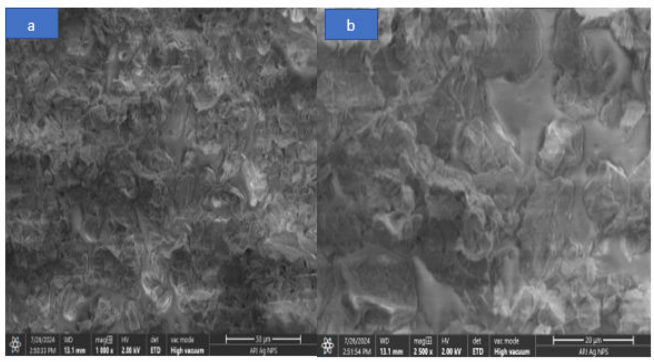

Figure 6: SEM analysis of biosynthesized Ag NPs: (A) at 1000 × magnification (B) at 2500 × magnification.

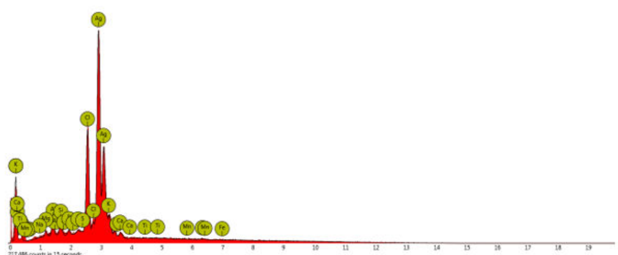

Figure 7: EDX analysis of biosynthesized Ag NPs.

Table 1: EDX analysis of biosynthesized Ag NPs.

Element number	Element symbol	Element name	Atomic conc.	Weight conc.
47	Ag	Silver	54.92	79.93
17	Cl	Chlorine	27.36	13.09
13	Al	Aluminum	5.42	1.97
14	Si	Silicon	3.38	1.28
12	Mg	Magnesium	3.62	1.19
20	Ca	Calcium	1.39	0.75
15	P	Phosphorus	1.55	0.65
26	Fe	Iron	0.62	0.47
16	S	Sulfur	0.76	0.33
11	Na	Sodium	0.79	0.25
19	K	Potassium	0.19	0.1
22	Ti	Titanium	0	0
25	Mn	Manganese	0	0

Transmission Electron Microscope (TEM) analysis

Transmission Electron Microscopy (TEM) was employed to evaluate the dimensions and structure of the produced Ag NPs. The TEM images, displayed in Figure 8 (a-c), revealed the creation of predominantly spherical nanoparticles with uniform size distribution [34]. Various magnifications were used to capture TEM images, enabling the identification of individual particles. The nanoparticles exhibited a range of sizes, with diameters spanning from 9.22 nm to 52.60 nm. Close examination of the TEM images revealed a subtle, thin coating of material on the Ag NPs' surface, potentially attributable to organic capping agents from *T.* cacao leaf extracts. While the synthesized Ag NPs demonstrated diverse shapes, most were spherical, with a small number of hexagonal formations also observed.

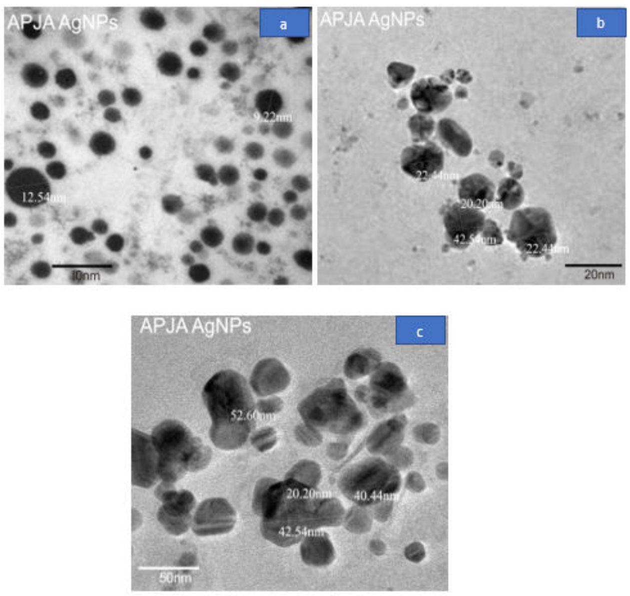

Figure 8: TEM analysis of synthesized Ag NPs.

Analysis of photocatalytic activity

The main factors responsible for the decolonization of dyes were hydroxyl and oxy radicals, which degrade toxic contaminants formed when a hole-electron pair was created. Furthermore, the color of dye simultaneously became lighter with time. When exposed to light energy, the indigo carmine dye's electrons become excited. These energized electrons interact with oxygen and water molecules, producing Reactive Oxygen Species (ROS).

The dye molecules then attach to the surface of silver nanoparticles. The generated ROS attack these attached dye molecules, decomposing them into smaller, less harmful compounds. While the silver nanoparticle achieves about 80.2% dye degradation, there is potential for enhancement. Several factors may contribute to the incomplete degradation: The photocatalytic activity of the silver nanoparticle might be insufficient to generate enough ROS for complete dye breakdown, the silver nanoparticle's surface area may not be adequate to adsorb all dye molecules, thereby limiting degradation efficiency, and other reactions occurring on the silver nanoparticle's surface could compete with the dye degradation process, reducing its effectiveness. The possible dye degradation mechanism is given below:

$$\text{Indigo carmine dye (IC)} + h\nu \rightarrow IC^{*} \quad (1)$$

$$IC^{*} + O_2 \rightarrow IC^{+} + {}^{\bullet}O_2^{-} \text{ (superoxide anion)} \quad (2)$$

$${}^{\bullet}O_2^{-} + H_2O \rightarrow {}^{\bullet}OH + OH^{-} \quad (3)$$

$$IC + {}^{\bullet}OH \rightarrow \text{Degraded IC Products} \quad (4)$$

Where, hν signifies the energy of light, IC* denotes the indigo carmine dye in its excited state, whilst $\bullet OH$ and $\bullet O_2^-$ represent the hydroxyl free radical and superoxide anion, respectively. The degradation efficiency for IC was 80.2% after 75 min of exposure to Uv-vis in the presence of a photocatalyst, as shown in Figures 9 and 10 and Table 2. The higher the rate constant, the faster the reaction rate and *vice versa*.

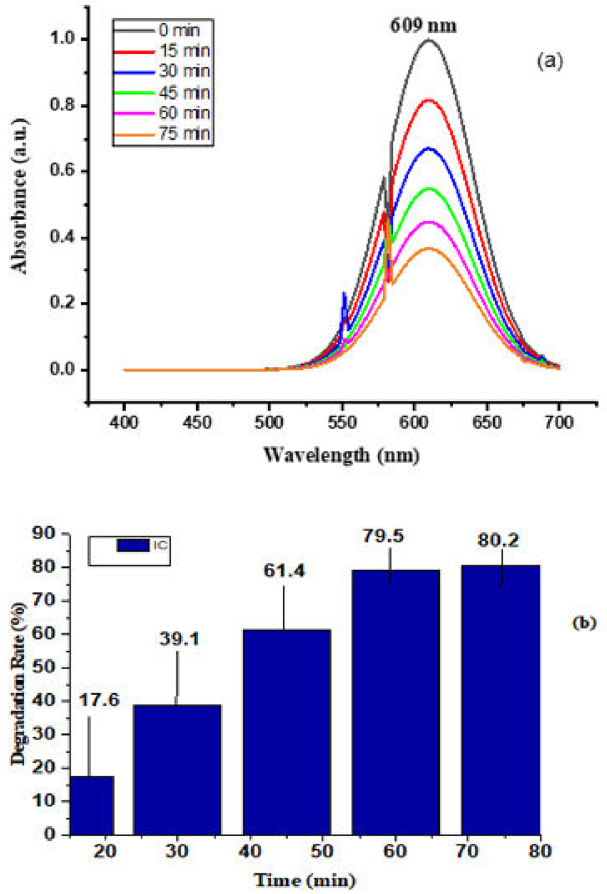

Figure 9: (A) Absorption spectra of the indigo carmine dye at different time intervals and (B) Degradation rate of Indigo Carmine (IC) dye.

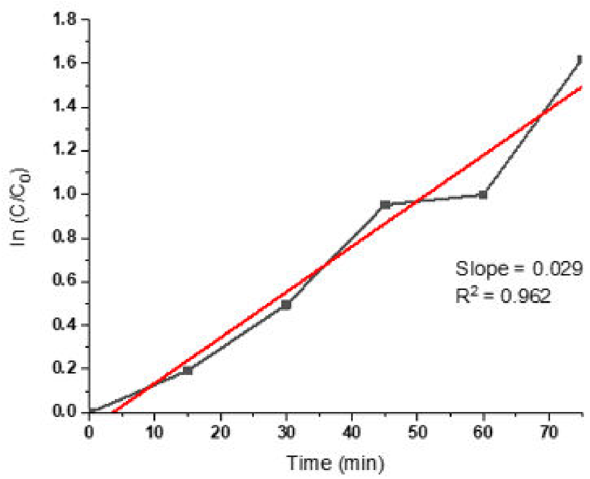

Figure 10: Kinetic results for indigo carmine dye degradation by Ag NPs.

Table 2: Comparing current work and previous studies for Ag NPs from wastes in photocatalytic activities against different pollutants.

Photocatalyst type	Sample	Waste type	Time (min)	Efficiency (%)	References
Ag NPs	*Bacillus amyloliquefaciens* (MSR5)	4-nitrophenol	15	98	[28]
$Ag/Ag_2O/P25$	*Capsicum annuum* L. (chili)	2,4 DNA	60	100	[35]
Ag NPs	Tulsi leaves	4-nitrophenol	30	100	[28]
Ag NPs	Coffee waste	Phenol			[1]
Ag NPs	*Thymbra spicata*/leaves	4-nitrophenol	1	96	[2]
Ag NPs	Coffee waste	2,4 DNA	30	97.7	[3]
Ag NPs	*Theobroma cacao*	Indigo carmine	75	80.2	Current work

CONCLUSION

The ecologically sound production of nanoparticles of silver employing *Theobroma cacao* leaf extract is being recognized as an intriguing path with a variety of potential, especially in the fields of sewage treatment and in the search for environmentally conscious and sustainable solutions. Utilizing Theobroma cacao, a plant famous for its many advantages, this novel method creates silver nanoparticles with astounding efficiency and ecological sustainability. Based on the results, the following conclusions were made.

According to FT-IR studies using an aqueous *T. cacao* leaf extract, plant-based nutrients such as proteins, flavonoids, alkaloid compounds, and phenolics, which act as surface-active substances, contributed to the stabilization of nanoparticles. These phytochemicals are associated with the outer layer of silver and play a role in stabilizing silver nanoparticles. XRD analysis revealed that the face-centered cubic plane of Ag NPs exhibited characteristic peak intensity patterns. TEM imaging of the Ag nanoparticles showed a size distribution ranging from 9.22 nm to 52.60 nm in diameter, with an average particle size of 28.52 nm determined through TEM analysis. The photocatalytic properties of the silver nanoparticles, specifically their ability to degrade harmful dyes in synthetic water, were evaluated through dye decomposition experiments. The findings indicate that the material achieved an 80.2% degradation efficiency at 75 minutes, with a half-life disintegration rate of 23.9 min^{-1}. These results suggest that the biosynthesis of silver nanoparticles using *T. cacao* leaf extract is highly suitable for treating industrial effluents, particularly those containing pigments.

To summarize, our research has illuminated the promise of eco-friendly silver nanoparticles derived from *Theobroma cacao* leaf extract in addressing wastewater treatment challenges. The study demonstrated that these synthesized Ag nanoparticles exhibit significant potential as photocatalysts for the swift degradation of industrial dyes during water purification processes. These nanoparticles could serve as a crucial asset in ongoing efforts to protect environmental and public health, underscoring the importance of sustainable nanotechnology in tackling current global issues. However, realizing this potential will require additional research and advancement.

REFERENCES

1. El-Kammah M, Elkhatib E, Gouveia S, Cameselle C, Aboukila E. Enhanced removal of indigo carmine dye from textile effluent using green cost-efficient nanomaterial: Adsorption, kinetics, thermodynamics and mechanisms. Sustain Chem Pharm. 2022;29:100753.
2. Adel M, Ahmed MA, Mohamed AA. Effective removal of indigo carmine dye from wastewaters by adsorption onto mesoporous magnesium ferrite nanoparticles. Environ Nanotechnol Monit Manag. 2021;16:100550.
3. Pereira PC, Reimão RV, Pavesi T, Saggioro EM, Moreira JC, Correia FV. Lethal and sub-lethal evaluation of Indigo Carmine dye and byproducts after TiO_2 photocatalysis in the immune system of *Eisenia andrei* earthworms. Ecotoxicol Environ Saf. 2017;143:275-282.
4. Assémian AS, Kouassi KE, Drogui P, Adouby K, Boa D. Removal of a persistent dye in aqueous solutions by electrocoagulation process: Modeling and optimization through response surface methodology. W, A & S Pollution. 2018;229:1-3.
5. Odogu AN, Daouda K, Keilah LP, Tabi GA, Rene LN, Nsami NJ, et al. Effect of doping activated carbon based *Ricinodendron heudelotti* shells with AgNPs on the adsorption of indigo carmine and its antibacterial properties. Arab J Chem. 2020;13(5):5241-5253.
6. Bożęcka A, Orlof-Naturalna M, Kopeć M. Methods of dyes removal from aqueous environment. J Ecol Eng. 2021;22(9).
7. Devatha CP, Jagadeesh K, Patil M. Effect of green synthesized iron nanoparticles by *Azardirachta indica* in different proportions on antibacterial activity. Environ Nanotechnol Monit Manag. 2018;9:85-94.
8. Raghavendra VB, Shankar S, Govindappa M, Pugazhendhi A, Sharma M, Nayaka SC. Green synthesis of zinc oxide nanoparticles (ZnO NPs) for effective degradation of dye, polyethylene and antibacterial performance in waste water treatment. J Inorg Organomet Polym Mater. 2022:1-7.
9. Abdelghaffar F. Biosorption of anionic dye using nanocomposite derived from chitosan and silver Nanoparticles synthesized *via* cellulosic banana peel bio-waste. Environ Technol Innov. 2021;24:101852.
10. Meher A, Tandi A, Moharana S, Chakroborty S, Mohapatra SS, Mondal A, et al. Hybrid Advances. 2024;6.

11. Dhaka A, Mali SC, Sharma S, Trivedi R. A review on biological synthesis of silver nanoparticles and their potential applications. Results Chem. 2023;6:101108.

12. Jadoun S, Arif R, Jangid NK, Meena RK. Green synthesis of nanoparticles using plant extracts: A review. Environ Chem Lett. 2021;19(1):355-374.

13. Dhaka A, Mali SC, Sharma S, Trivedi R. A review on biological synthesis of silver nanoparticles and their potential applications. Results Chem. 2023;6:101108.

14. Ong WT, Nyam KL. Evaluation of silver nanoparticles in cosmeceutical and potential biosafety complications. Saudi J Biol Sci. 2022;29(4):2085-2094.

15. Kwon YM, Cho ES, Kim KW, Chung D, Bae SS, Yu WJ, et al. Synthesis of silver nanoparticles using *Aggregatimonas sangjinii* F202Z8T and their biological characterization. Microorganisms. 2023;11(12):2975.

16. Hublikar LV, Ganachari SV, Patil VB, Nandi S, Honnad A. Anticancer potential of biologically synthesized silver nanoparticles using *Lantana camara* leaf extract. Prog Biomater. 2023;12(2):155-169.

17. Shankar SS, Rai A, Ahmad A, Sastry M. Rapid synthesis of Au, Ag, and bimetallic Au core–Ag shell nanoparticles using Neem (*Azadirachta indica*) leaf broth. J Colloid Interface Sci. 2004;275(2):496-502.

18. Schneidewind H, Schüler T, Strelau KK, Weber K, Cialla D, Diegel M, et al. The morphology of silver nanoparticles prepared by enzyme-induced reduction. Beilstein J Nanotechnol. 2012;3(1):404-414.

19. Sulaiman GM, Mohammed WH, Marzoog TR, Al-Amiery AA, Kadhum AA, Mohamad AB. Green synthesis, antimicrobial and cytotoxic effects of silver nanoparticles using *Eucalyptus chapmaniana* leaves extract. Asian Pac J Trop Biomed. 2013;3(1):58-63.

20. Kouvaris P, Delimitis A, Zaspalis V, Papadopoulos D, Tsipas SA, Michailidis N. Green synthesis and characterization of silver nanoparticles produced using *Arbutus unedo* leaf extract. Mater Lett. 2012;76:18-20.

21. Kumar A, Kumar M, Jose A, Tomer V, Oz E, Proestos C, et al. Major phytochemicals: Recent advances in health benefits and extraction method. Molecules. 2023;28(2):887.

22. Patil S, Sivaraj R, Rajiv P, Venckatesh R, Seenivasan R. Green synthesis of silver nanoparticle from leaf extract of *Aegle marmelos* and evaluation of its antibacterial activity. Int J Pharm Pharm Sci. 2015;7(6):169-173.

23. Mahiuddin M, Saha P, Ochiai B. Green synthesis and catalytic activity of silver nanoparticles based on *Piper chaba* stem extracts. Nanomaterials. 2020;10(9):1777.

24. de Souza DC, Matos VA, dos Santos VO, Medeiros IF, Marinho CS, Nascimento PR, et al. Effects of high-intensity interval and moderate-intensity continuous exercise on inflammatory, leptin, IgA, and lipid peroxidation responses in obese males. Front Physiol. 2018;9:567.

25. Rodríguez-Félix F, Graciano-Verdugo AZ, Moreno-Vásquez MJ, Lagarda-Díaz I, Barreras-Urbina CG, Armenta-Villegas L, et al. Trends in Sustainable green synthesis of silver nanoparticles using agri-food waste extracts and their applications in health. J Nanomater. 2022;2022(1):8874003.

26. Abbas R, Luo J, Qi X, Naz A, Khan IA, Liu H, et al. Silver nanoparticles: Synthesis, structure, properties and applications. Nanomaterials. 2024;14(17):1425.

27. Ghubish Z, Kamal R, Mahmoud HR, Saif M, Hafez H, El-Kemary M. Photocatalytic activation of Ag-doped $SrSnO_3$ nanorods under visible light for reduction of p-nitrophenol and methylene blue mineralization. J Mater Sci Mater Electron. 2022;33(31):24322-24339.

28. El-Desouky N, Shoueir K, El-Mehasseb I, El-Kemary M. Synthesis of silver nanoparticles using bio valorization coffee waste extract: Photocatalytic flow-rate performance, antibacterial activity, and electrochemical investigation. Biomass Convers Biorefin. 2023;13(17):15871-15885.

29. El-Shabasy R, Yosri N, El-Seedi H, Shoueir K, El-Kemary M. A green synthetic approach using chili plant supported Ag/Ag_2O@ P25 heterostructure with enhanced photocatalytic properties under solar irradiation. Optik. 2019;192:162943.

30. Sengupta A, Sarkar A. Synthesis and characterization of nanoparticles from neem leaves and banana peels: A green prospect for dye degradation in wastewater. Ecotoxicology. 2022;31(4):537-548.

31. Thatikayala D, Jayarambabu N, Banothu V, Ballipalli CB, Park J, Rao KV. Biogenic synthesis of silver nanoparticles mediated by T*heobroma cacao* extract: Enhanced antibacterial and photocatalytic activities. J Mater Sci Mater Electron. 2019;30:17303-13.

32. Miri A, Shahraki Vahed HO, Sarani M. Biosynthesis of silver nanoparticles and their role in photocatalytic degradation of methylene blue dye. Res Chem Intermed. 2018;44:6907-6915.

33. Samuel MS, Jose S, Selvarajan E, Mathimani T, Pugazhendhi A. Biosynthesized silver nanoparticles using *Bacillus amyloliquefaciens*; Application for cytotoxicity effect on A549 cell line and photocatalytic degradation of p-nitrophenol. J Photochem Photobiol B. 2020;202:111642.

34. Singh J, Mehta A, Rawat M, Basu S. Green synthesis of silver nanoparticles using sun dried tulsi leaves and its catalytic application for 4-Nitrophenol reduction. J Environ Chem Eng. 2018;6(1):1468-1474.

35. Veisi H, Azizi S, Mohammadi P. Green synthesis of the silver nanoparticles mediated by *Thymbra spicata* extract and its application as a heterogeneous and recyclable nanocatalyst for catalytic reduction of a variety of dyes in water. J Clean Prod. 2018;170:1536-1543.